Biophysical Journal, Volume *110*

Supplemental Information

Revealing Assembly of a Pore-Forming Complex Using Single-Cell Kinetic Analysis and Modeling

Mirko Bischofberger, Ioan Iacovache, Daniel Boss, Felix Naef, F. Gisou van der Goot, and Nacho Molina

Supporting Material:
Revealing assembly of a pore forming complex using single-cell kinetic analysis and modeling

M. Bischofberger, I. Iacovache, D. Boss,
F. Naef, F. G. van der Goot* and N. Molina*

SUPPORTING FIGURES:

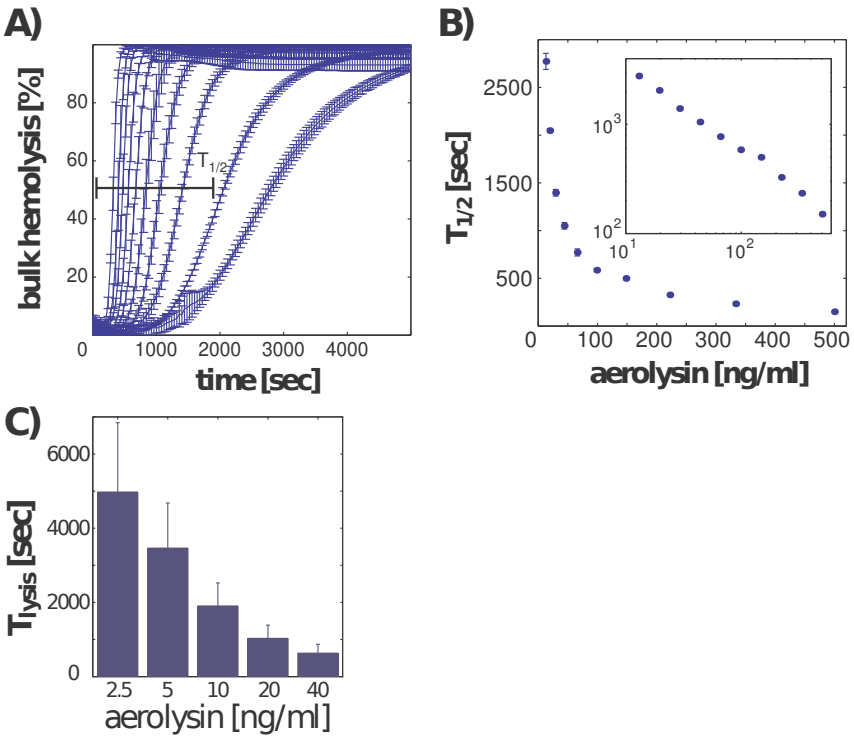

Figure S1. Bulk hemolysis with aerolysin. A) Red blood cells were treated with a serial dilution of 13-500ng/ml aerolysin and the absorbance at 450nm was recorded over time. Average of triplicates are shown. **B)** Half maximal lysis times in function of different initial aerolysin concentrations. *Inset:* Log-log plot. **C)** Spherization times extracted from the single-cell for different initial concentrations of aerolysin.

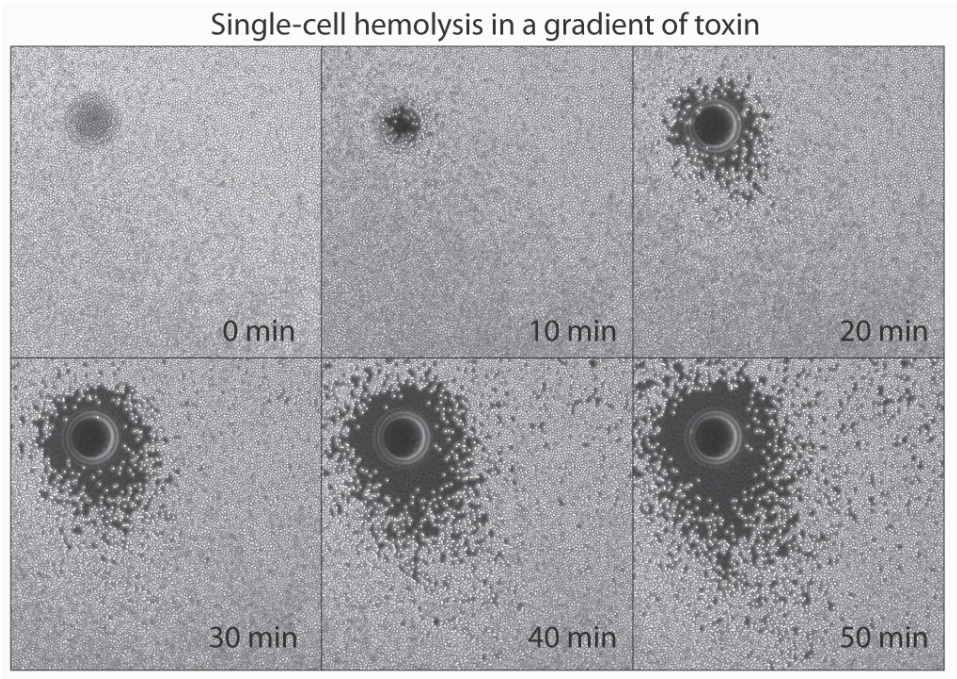

Figure S2. Stochastic lysis of erythrocytes in a gradient of toxin. A) Images of a lawn of erythrocytes at 0, 19, 20, 30, 40 and 50 minutes after the aerolysin-soaked bead exposure (dark circle in the upper-left corner). **B)** Light intensity as function of time and radial distance from the aerolysin-soaked bead.

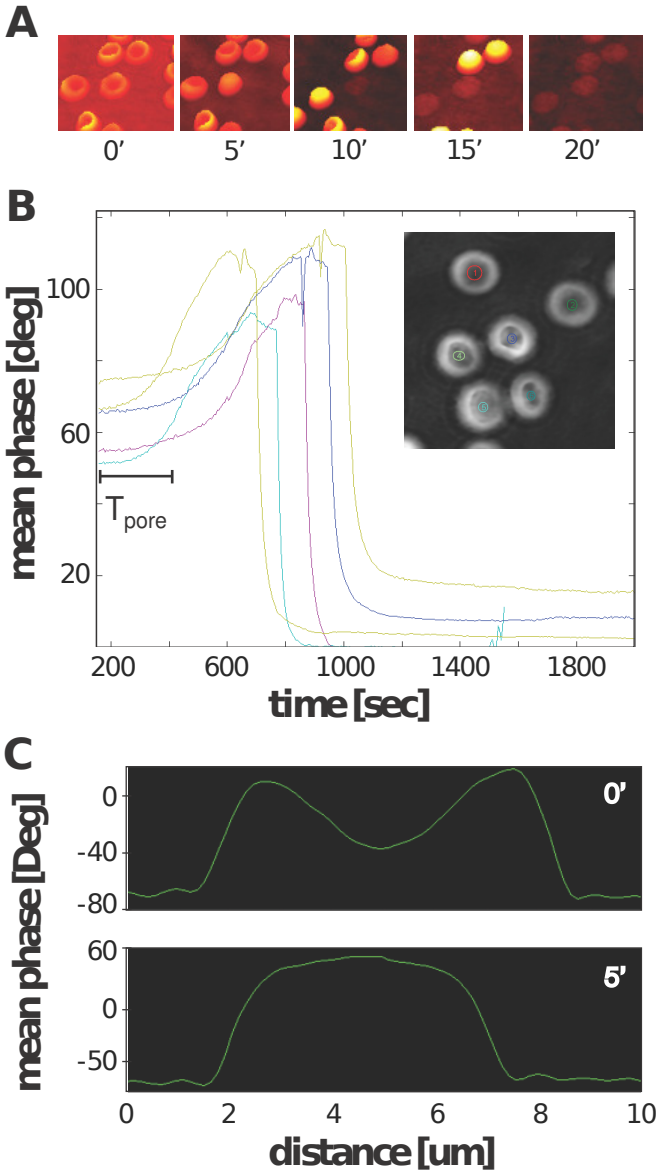

Figure S3. Digital holographic microscopy of erythrocytes treated with aerolysin. **A)** Surface reconstruction of a subset of red blood cells treated with 50ng/ml of aerolysin. **B)** Representative single-cell traces for 5 different cells. **C)** Cross section of a red blood cell at time t=0 min and at time t=5min.

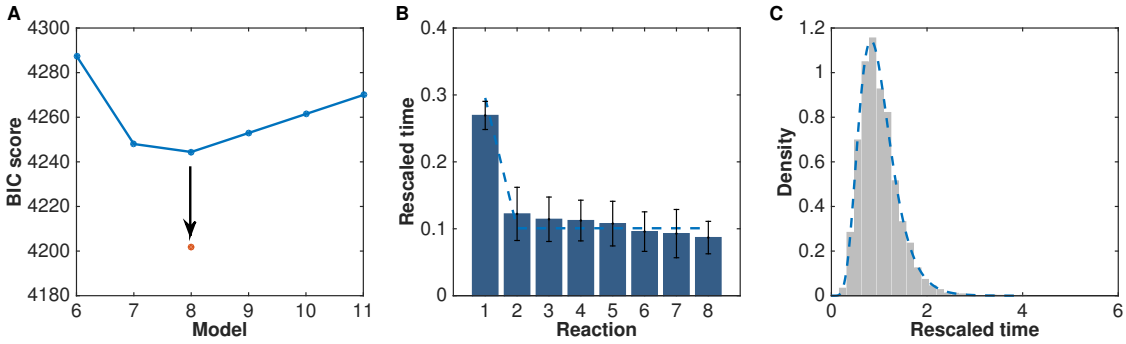

Figure S4. Test of the inference procedure on simulated data from a 7eq+1 model. A) BIC scores of models with reactions of different rates (blue) or with *n* reactions of equal rates plus an additional reaction (red dots). **B)** Posterior mean reaction times (bars) and posterior standard deviation (error bars) of an N=8 different reaction model computed via MCMC sampling. Dashed line represents the fitted reaction times of a 7eq+1 reaction model. **C)** Fit of a 7eq+1 reaction model (dashed line) to the rescaled pore formation lag times (bars).

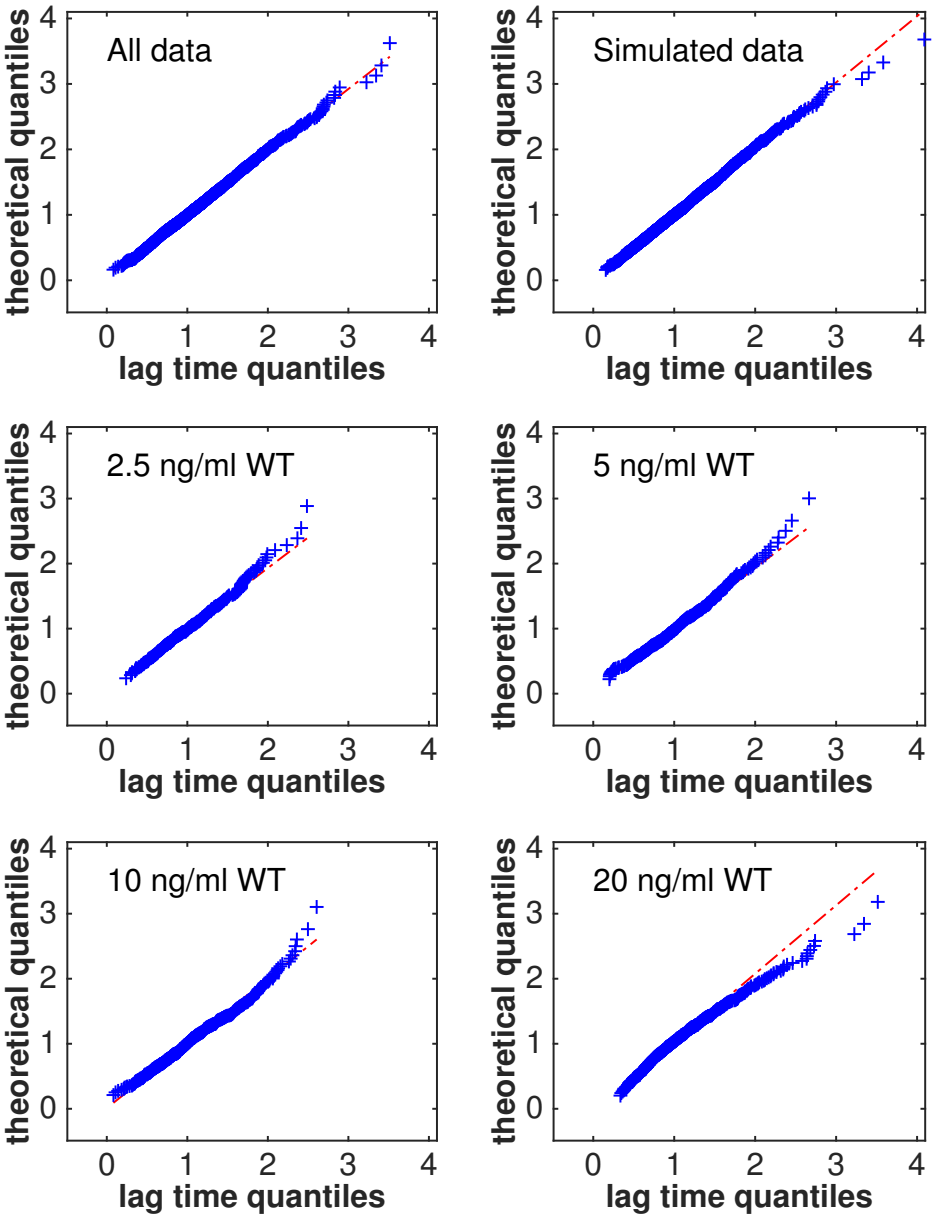

Figure S5. Quantile-quantile plots. A, B) Quantile-quantile plots of the pore formation lag time distributions of aerolysin against the fits of 7eq+1 model distributions with N=8 (see main text).

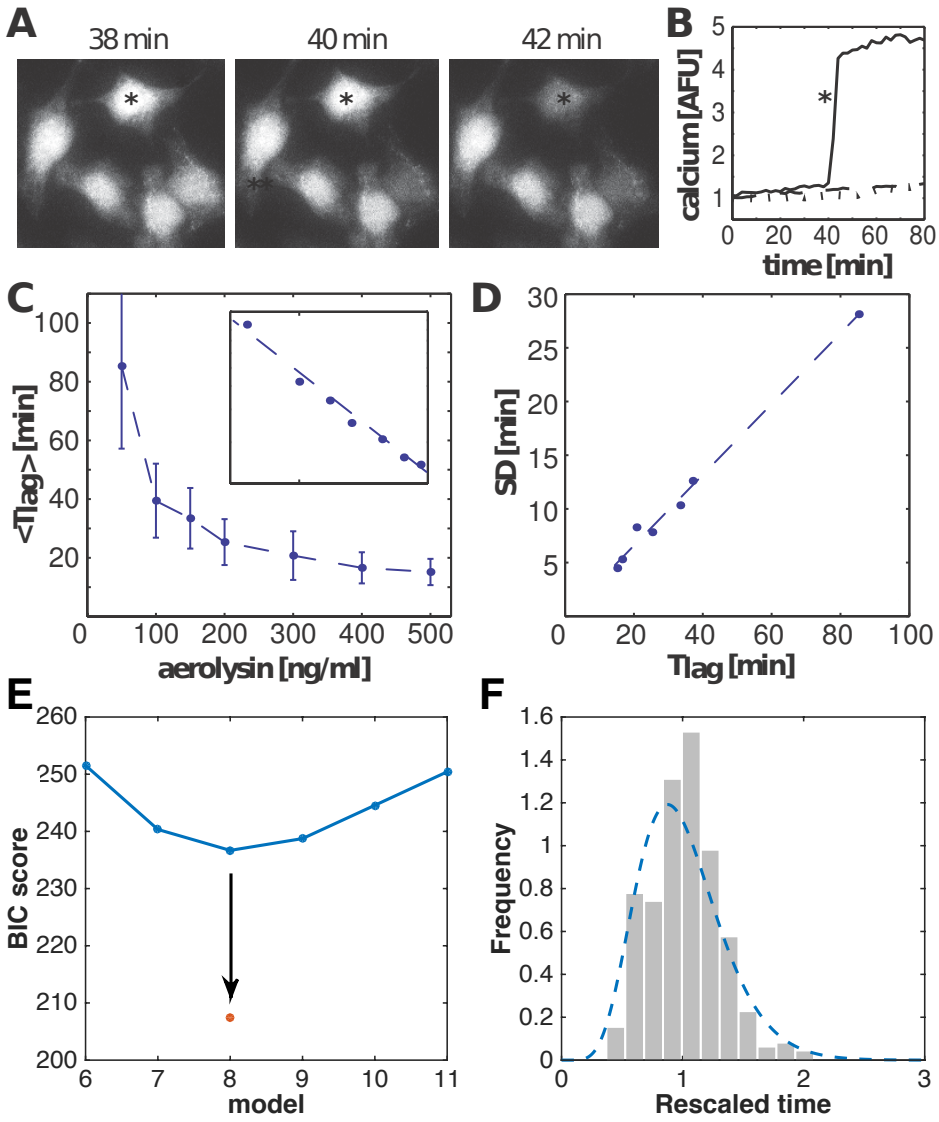

Figure S6. Pore formation lag times in nucleated cells. A) Thapsigargin treated-HeLa cells loaded with the calcium-sensitive dye Fura-FF, imaged every 2 minutes after aerolysin (100 ng/ml) treatment. **B)** Example of calcium influx in a cell from A) upon pore formation. No calcium increase is observed upon treatment with the pore formation mutant Y221G (dotted line) or without toxin (dashed line). **C)** Signature of pore formation time T_{lag} versus initial toxin concentration. *Inset:* Log-log plot. **D)** Linear scaling of standard deviation (SD) in function of mean pore formation times T_{lag}. **E)** BIC scores of models with reactions of different rates (blue) or with 7 reactions of equal rates plus an additional reaction (red dot). **F)** Distribution of rescaled lag times for aerolysin fitted to a 7eq+1 model distribution.

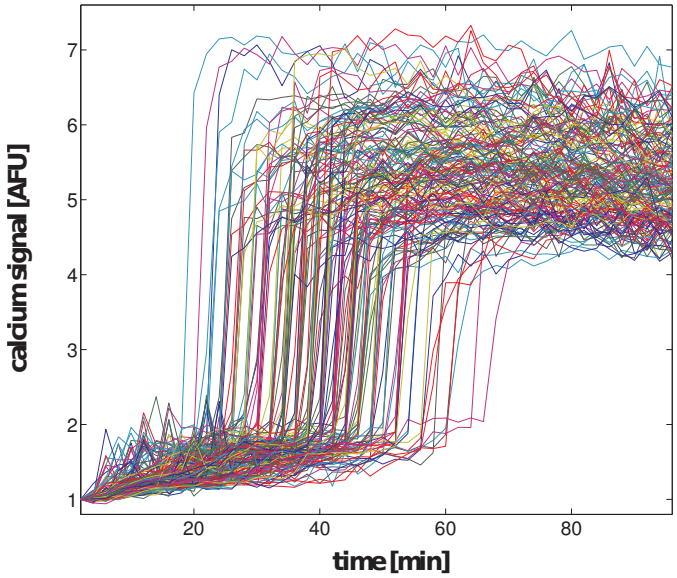

Figure S7. Calcium traces of aerolysin-treated HeLa cells. Subset of single-cell traces obtained for HeLa cells loaded with the calcium-sensitive dye Fura-FF and challenged with 100 ng/ml of aerolysin.